EasyChair Preprint

№ 9105

Frequency Interleaved DAC System Design: Fundamental Problems and Compensation Methods

Nagito Ishida, Koji Asami, Shogo Katayama, Anna Kuwana and Haruo Kobayashi

October 24, 2022

Frequency Interleaving DAC System Design: Fundamental Problems and Compensation Methods

Nagito Ishida[1,a], Koji Asami[2,b], Shogo Katayama[1,c], Anna Kuwana[1,d], Haruo Kobayashi[1,e]

[1] Gunma University 1-5-1 Tenjin-cho Kiryu Gunma 376-8515, Japan
[a] t190d011@gunma-u-ac.jp, [c] t15304906@gunma-u-ac.jp, [d] kuwana.anna@gunma-u-ac.jp, [e] koba@gunma-u-ac.jp

[2] Advantest Corporation, Japan
[b] koji.asami@advantest.com

Abstract. This paper describes wideband digital-to-analog conversion circuits (DACs) using frequency interleaving architecture. Along with broadband communication standards, wideband DACs are required for wideband communication device measurement and test equipment. First, we explain the basic configuration and operation of the frequency interleaving DAC (FI-DAC) architecture. There the digital input signal is divided into multiple bands. Then they are demodulated and provided to several sub-DACs, whose analog outputs are modulated and synthesized to the wideband analog output signal. Note that image components are generated by sub-DACs and modulations, which have to be removed by subband synthesis analog filters. The other fundamental problems of this architecture are signal attenuation by zero-th order hold of each sub-DAC output, phase-nonlinearity characteristic of synthesis analog filters, group delay differences among subband channels, and phase discontinuity between adjacent subband channels. We examine compensation methods for these problems, and their effectiveness is confirmed with MATLAB simulation.

Keywords: DAC, frequency interleaving, wideband signal generation, modulation, broadband

1 Introduction

Communication standards have been changing from 4G to 5G, and furthermore 6G is being considered; they are becoming increasingly wideband. Therefore, wideband measuring instruments are required to measure and test these devices. As one of the methods for realizing a wideband ADC, interleaved ADCs using multiple channels such as time-interleaved ADC (TI-ADC) [1] and frequency-interleaved ADC (FI-ADC) [2],[3],[4] have been investigated for a long time. Recently, research has begun to apply the interleaving techniques to DACs, and similarly there are two interleaving methods: time interleaved DACs (TI-DACs) and frequency interleaved DACs (FI-DACs).

The concept of the TI-DAC is to combine the output signals of multiple DACs whose output timings are shifted each other, but sampling timings are the same, and which are combined in the time domain [5][6], whereas that of the FI-DAC is to combine the

output signals of multiple DACs whose covering bandwidths are different each other in output [7][8]. The TI-DAC has a limitation to increase the number of channels; analog switches for their output multiplexing are difficult to realize in case of the wideband DAC, [9].therefore it is difficult to realize a wideband TI-DAC by zero-th order hold. On the other hand, since the FI-DAC is not restricted by the sub-DAC zero-th order hold output characteristic, the number of channels can be increased for the wideband signal generation There the removal of Nyquist image by interleaving has been also investigated [10][11].

The FI-DAC is a novel concept proposed in recent decades, and several approaches and compensation methods have been proposed as follows:(i) The FI-DAC has the interdependencies between the bandwidth, the sample rate, the number of samples and the frequencies of the local oscillators (LOs). In order to balance the interdependent system parameters, a mathematical optimization approach is introduced in the form of two mixed-integer nonlinear optimization programs (MINLPs) [8]. (ii) A closed algebraic expression for the distribution of the data samples among the DACs is shown in order to realize guard bands suppressing DAC aliases and unused mixer side bands [12]. (iii) As their compensation method, a multiple-input multiple-output (MIMO) digital signal processing (DSP) algorithm to avoid the crosstalk between the frequency bands has been devised [13]. There DSP for frequency domain equalization utilizes a repetitive data sequence. (iv) A compensation method using a MIMO equalizer and a backpropagation algorithm by adapting its coefficients has been developed [14][15].

In this paper, we investigate to compensate for FI-DAC fundamental problems using digital and analog filters and adjusting the initial phases of the carriers. The organization of this paper is as follows. First, we explain the basic configuration and operation of the FI-DAC architecture. We show image component generation by modulation and DAC output zero-th order hold. Next, we explain signal attenuation by the DAC and phase characteristic of digital and analog filters. Then we describe their compensation methods using digital signal processing [16][17]. They are summarized in Table 1. Finally, MATLAB simulation results of these compensations are shown for their verification.

Table1 Fundamental problems and their compensations

Problems	Compensation methods
Signal attenuation by DAC zero-th order hold output	Applying an inverse sinc filter
Phase-nonlinearity characteristic of smoothing and synthesis analog filters	Applying all-pass filters
Differences in group delay among subband channels	Changing the sampling timing
Phase discontinuity between adjacent subband channels	Adjusting the initial phase of the carrier signal in digital signal processing

2 Principle and structure of FI-DAC Architecture

2.1 FI-DAC Architecture

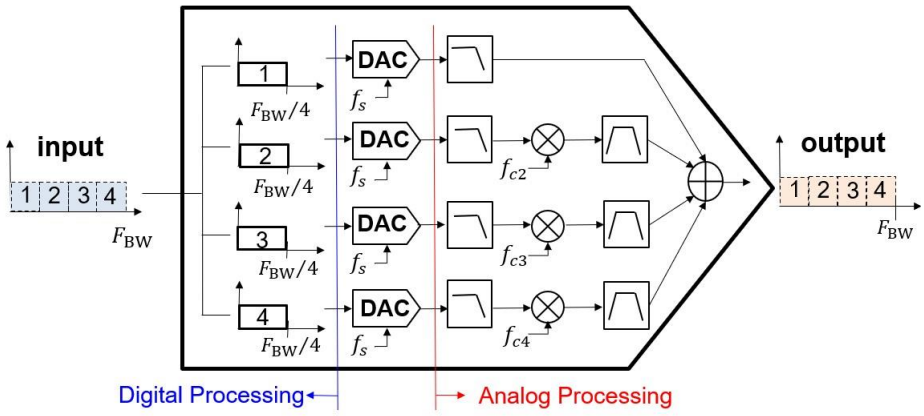

Fig. 1. Structure of the investigated 4-channel FI-DAC architecture

Fig.1 shows the investigated structure of the 4-channel FI-DAC. First, the input signal band is divided into four subband channels by digital signal processing. Second, each corresponding sub-DAC provides the output for each band. Third, these output signal bands are shifted back to the targeted signal band using analog modulation. Finally, the outputs of all subband channels are combined.

Here F_{BW} denotes the input signal band, f_s does the sampling frequency of sub-DACs, k does the number of channels, and f_{ck} does the carrier frequency of the k-th subband channel. In this structure, we have the following relationship between the sampling frequency and the output signal band:

$$\frac{f_s}{2} \geq \frac{F_{BW}}{4} \tag{1}$$

In case of M- subband channel, we have the following:

$$\frac{f_s}{2} \geq \frac{F_{BW}}{\mathrm{M}} \tag{2}$$

2.2 Generation of image components

Image components by DAC zero-th order hold output

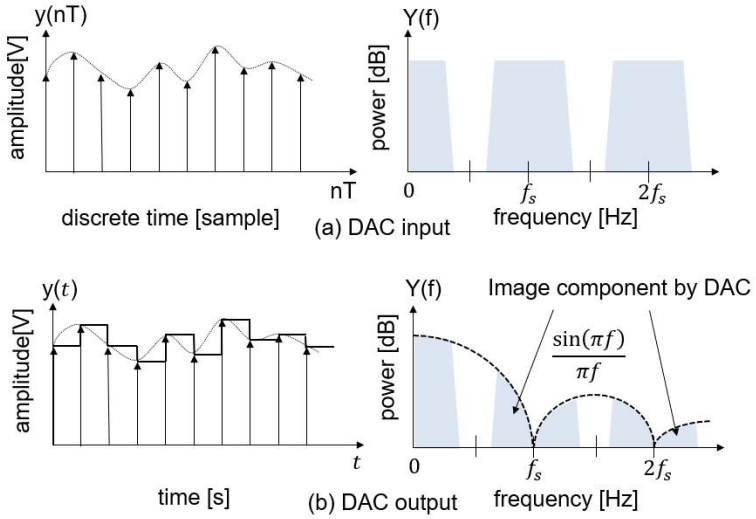

Fig. 2. DAC output with zero-th order hold

Fig. 2 shows input and output signal waveforms and power spectrum of a zero-th order hold DAC. In Fig.4, (a) shows the DAC input, while (b) does the DAC output. Image components are generated in the input, and their spectrum are mirrored with respect to $f_s/2$. Besides, the signal spectrum power has the attenuation tendency for higher frequency in output. Image components have to be removed by the following synthesis analog lowpass filter as shown in Fig. 3. This filter is called as smoothing analog filter.

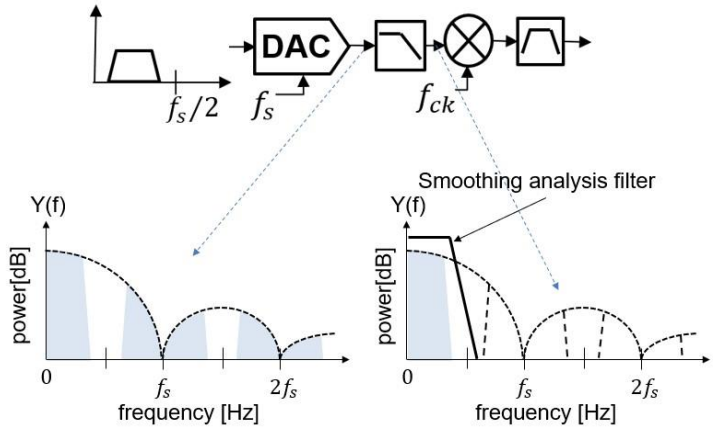

Fig. 3. Removal of image components caused by DAC zero-th order output using smoothing analog filter.

Image components generated by modulation

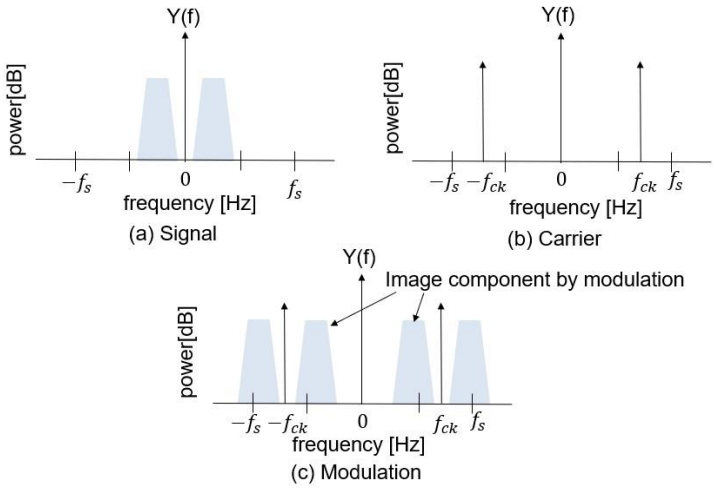

Fig. 4. Image components generated by modulation

Fig.4 shows the process of generating image components by the amplitude modulation (AM) on the frequency axis.

In Fig.4, (a) shows the signal spectra, and (b) shows carrier spectra, while (c) shows the modulated signal spectra. The signal spectrum is shifted to the carrier frequency by the AM, and the image components appear in the lower side of the carrier frequency, as shown in Fig.4. (c). In FI-DAC, they can be removed by the analog bandpass filter followed by the mixer as shown in Fig. 5.

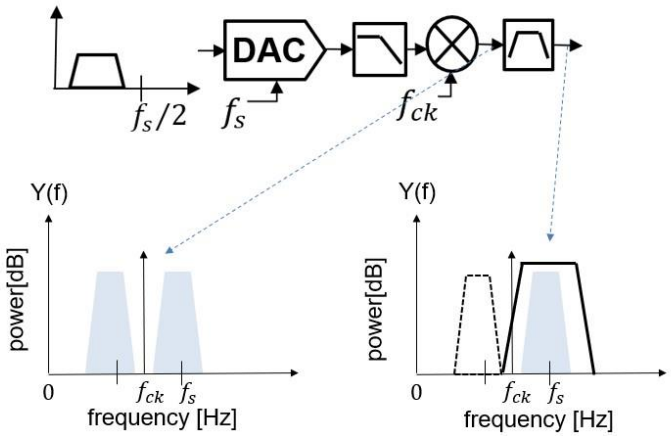

Fig. 5. Removal of image components caused by modulation using the analog band-pass filter.

Restriction of signal bandwidth input to sub-DAC

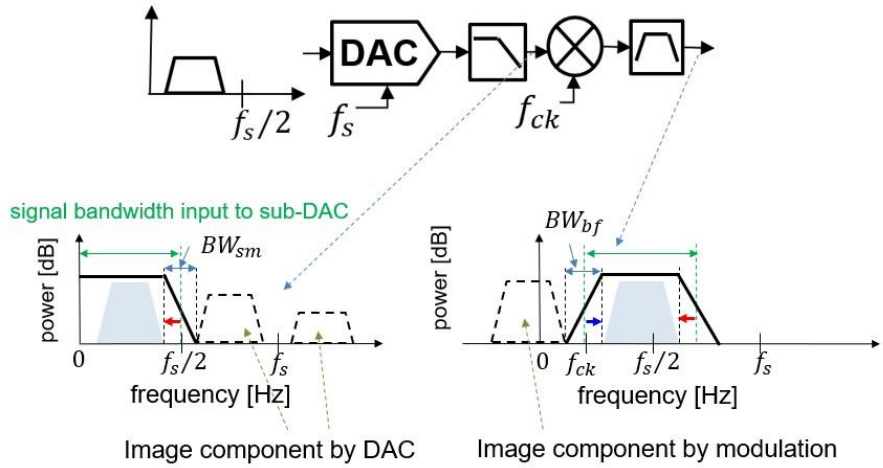

Fig. 6. Restriction of signal bandwidth input to sub-DAC by DAC zero-th order output and modulation.

The input signal bandwidth to sub-DAC is between 0 and $f_s/2$. Since the image components shown in Figs. 2 and 4 degrade the overall FI-DAC output signal quality, they have to be removed by synthesis analog filters. Since the filter has the transition band between the signal component and the image component, the frequency interval corresponding to the transition bandwidth has to be secured. For this reason, the input band becomes narrower than that between 0 to $f_s/2$, as shown in Fig. 6. There BW_{sm} is the transition bandwidth of the smoothing analog lowpass filter and BW_{bf} is that of the synthesis analog bandpass filter. The image components are generated by the DAC and they are mirrored with respect to $f_s/2$, so the signal bandwidth becomes narrower; it yields from $f_s/2$ to $BW_{sm}/2$. The image components are generated by modulation and they are mirrored with respect to f_{ck}, and the signal bandwidth narrows; it is from 0 to $BW_{bf}/2$. Accordingly, the signal bandwidth is expressed as follows:

$$\frac{BW_{bf}}{2} \leq \text{signal bandwidth input to sub-DAC} \leq \frac{f_s}{2} - \frac{BW_{sm}}{2} \tag{3}$$

2.3 Subband analysis digital signal processing

Overall block diagram of subband analysis digital signal processing

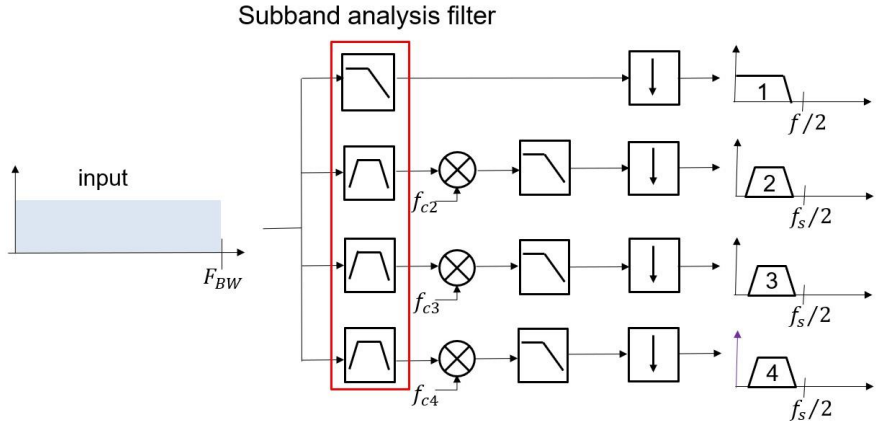

(a) Block diagram of subband analysis digital signal processing.

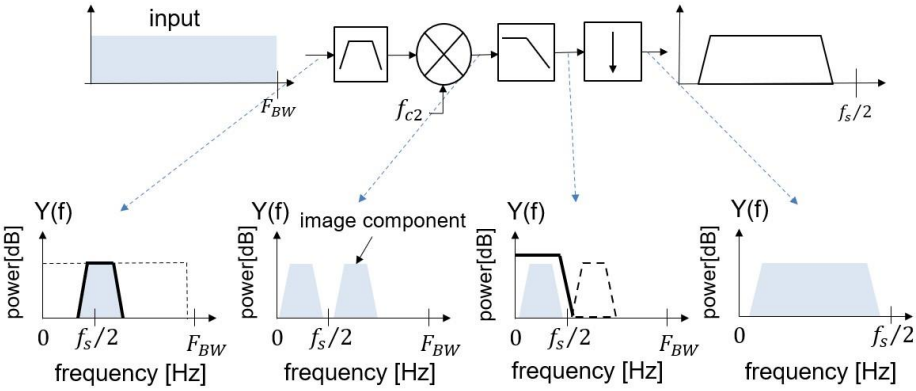

(b) Subband channel analysis digital signal processing.

Fig. 7. Subband analysis digital filter processing.

Fig. 7 shows digital signal processing for the sub-DAC input. In Fig. 7, (a) shows the block diagram from the input to the sub-DAC input, while (b) shows the power spectrum of each processing. The input signal is split in frequency domain using analysis digital filters surrounded by the red frame in Fig. 7 (a), and the frequency shift is performed for the bands to be within $0\sim f_s/2$. However, 1st-subband channel is already in the band $0\sim f_s/2$, so the frequency shift is not required. The image components by frequency shift are generated at subband channels 2, 3 and 4, and they have to be removed by analysis digital filters. Finally, the sampling rate is converted from the sampling frequency of the input to the sampling frequency of the sub-DAC.

Design of subband analysis digital filters

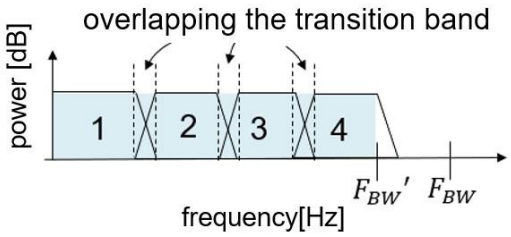

Fig. 8. Design of subband analysis digital filters

Fig. 8 shows the design specifications of the subband analysis digital filters used in Fig. 7 (a). We see that each analysis digital filter has a transition band. Therefore, by overlapping the transition bands between adjacent filters, they are designed so that signals in the bands inside the dotted lines in Fig. 8 are not attenuated at the final output. The signal band must satisfy equation (3). Fig. 9 shows the image components generated in case of the signal in the vicinity of F_{BW}. When the signal is frequency-shifted, the split band is moved from the original frequency by f_{ck}. An image component is generated close together, so it cannot be completely removed by the following filter; therefore, the overall FI-DAC output quality decreases. The overall DAC output band should be a little narrower than F_{BW} , which is defined as F_{BW}'.

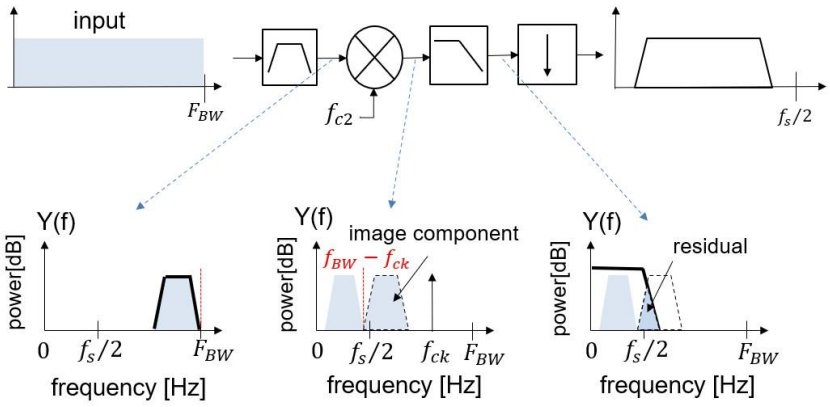

Fig. 9. Restriction of subband analysis digital filter.

3 Fundamental problems of FI-DAC architecture in principle and their compensation

3.1 Signal attenuation by DAC zero-th order hold output and its compensation method

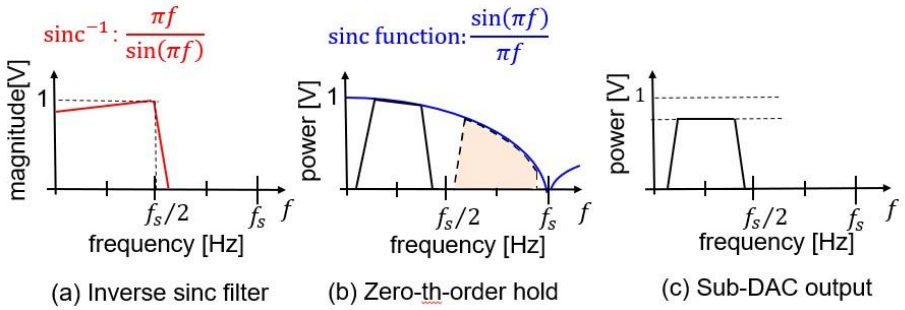

Fig. 10. Compensation of signal attenuation caused by DAC zero-th order hold output.

As mentioned in Section 2.2, the DAC output has zero-th order hold characteristic. So, the gain of the sub-DAC should be compensated to be flat over the signal band by using a pre-digital filter having the inverse gain characteristic of the sinc filter as shown in Fig.10 (a). In this way, even if the filter coefficients are normalized to the largest value, the dynamic range of the DAC output is reduced. Then, the amplitude of the output is reduced from the signal bandwidth input to sub-DAC. This loss can be compensated by the FI-DAC output amplifier.

3.2 Problems of phase characteristic and their compensation

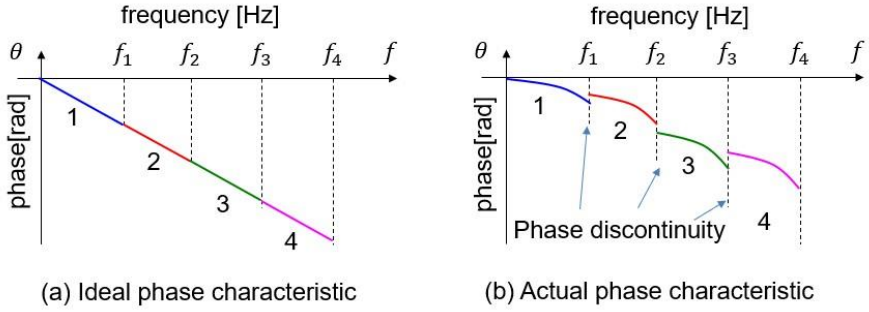

Fig. 11. Overall DAC output phase characteristic.

Fig. 11(a) shows the ideal overall DAC output phase characteristic which is completely linear. However, the actual phase characteristic for 4-channel FI-DAC tends to

be degraded, as shown in Fig. 11(b), which leads to the output waveform distortion. The causes of such phase characteristic degradation are as follows:

1 Phase-nonlinearity characteristic of synthesis analog filters
2 Differences in group delay among subband channels
3 Phase discontinuity between adjacent subband channels

Now we describe their compensation methods.

Phase-nonlinearity characteristic of smoothing and synthesis analog filters and their compensation

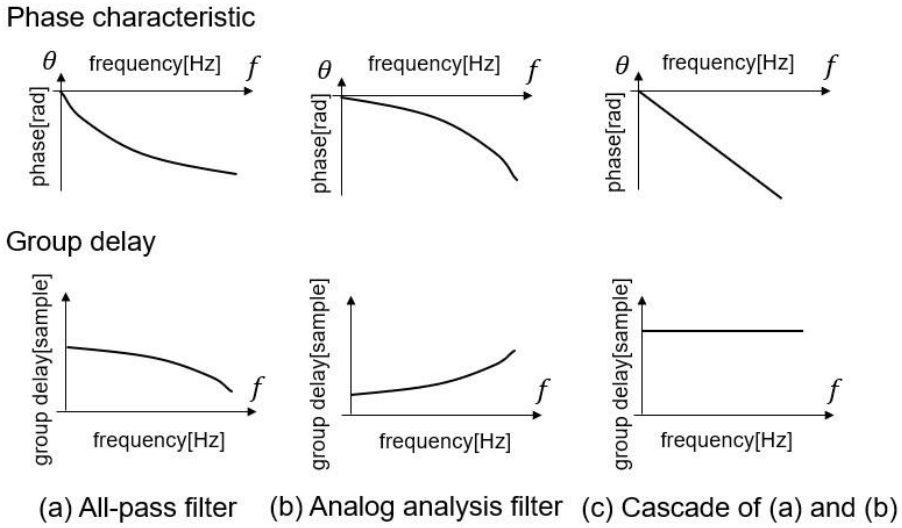

Fig. 12. Compensation for phase-nonlinearity characteristic of smoothing and synthesis analog filters.

The phase-nonlinearity of the smoothing and synthesis analog filter can be compensated using the all-pass filter. In Fig.12, (a) shows phase characteristic of the all-pass filter for the compensation and (b) shows phase characteristic of an analog filter, while (c) shows phase characteristic of cascade of these filters. Due to the phase-nonlinearity characteristic of the smoothing and synthesis analog filters, the group delay varies depending on the frequency. Therefore, an all-pass filter is used to perform group delay compensation [18].

Differences in group delay among subband channels and their compensation

As mentioned above, they can be compensated so that the group delay of the analog filter is constant in the entire band. However, the group delay of the filter by the compensation is different for each subband channel. In addition, since the first subband

channel has a filter of a small order than the other subband channels, the group delay by the filter is small. Therefore, the group delay is different among subband channels, and some distortion appears in the overall DAC output waveform. To compensate the group delay, we investigate the sampling timing adjustment for each subband channel to compensate for the group delay differences among subband channels.

Phase discontinuity between adjacent subband channels and their compensation

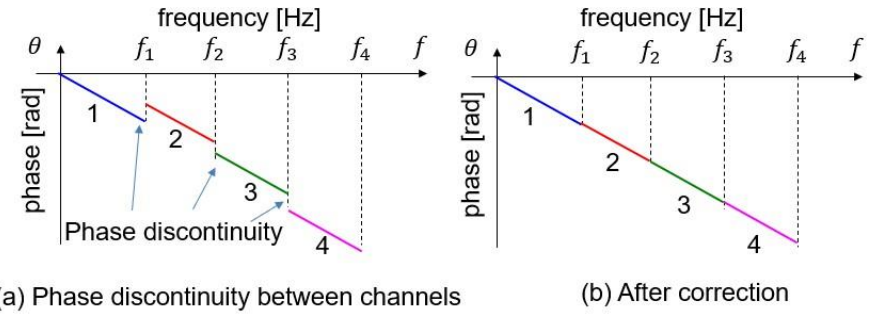

Fig. 13. Compensation of phase discontinuity between adjacent subband channels

In Fig. 13, (a) shows the phase characteristic compensated only by phase-nonlinearity characteristic of synthesis analog filters and differences in group delay among subband channels, and (b) shows the one with also phase discontinuity compensation. In this system, signal band changes by modulation and frequency shift. Filtering when changing from the original band causes an extra rotation of phase. In Fig. 13 (a), the phase for each subband channel is linear, but phase differences exist between adjacent subband channels, and the phase characteristic is discontinuous. This can be compensated by adjusting the initial phase of the carrier signal in digital signal processing. Let x(n) be a signal, $\cos(2\pi f_c n + \theta)$ be a carrier. A signal by frequency shift is calculated from multiplying x(n) by $\cos(2\pi f_c n + \theta)$. Then Discrete Fourier Transform (DFT) of x(n)$\cos(2\pi f_c n + \theta)$ is given as follows:

$$\sum_{n=0}^{N-1} x(n)\cos(2\pi f_c n + \theta) = \frac{1}{2}\left(\exp(j\theta)\,X(k+p) + \exp(-j\theta)\,X(k-p)\right) \tag{4}$$

where $X(k)$ is DFT of x(n), $f_c = p/N$ is the carrier frequency in digital signal processing, N is the number of the sampled data points, and p is a natural number satisfying $p = f_c N$. x(n) has both upper and lower sideband frequency components because of frequency shift. Based on the initial phase, the high-frequency component rotates by θ and the low-frequency component rotates by $-\theta$. As shown in the third power spectrum from the left in Fig. 7 (b), since the high-frequency component is removed by a low-pass filter, the signal components are only at low-frequency. That is, by giving the initial phase θ, the signal phase can be rotated by $-\theta$. As a result, the phases between adjacent subband channels become continuous as shown in Fig. 13 (b).

Fig. 14 shows the block diagram with the compensation described in this section.

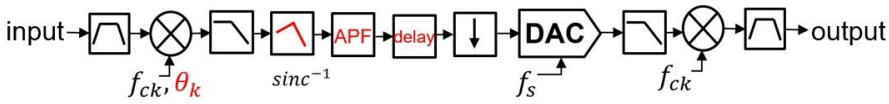

Fig. 14. Block diagram with compensations.

4 MATLAB Simulation

4.1 Simulation Conditions

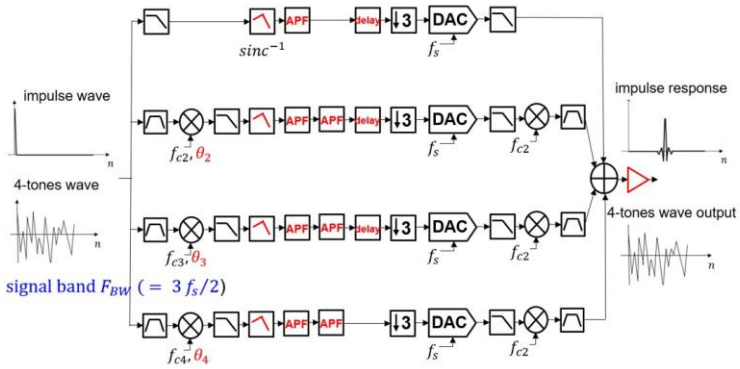

Fig. 15. Simulation block diagram

We have conducted MATLAB simulation to show the validity of the compensation methods for these problems. Fig. 15 shows a block diagram of simulation, and the compensations are shown in red there. F_{BW} is signal band of the input, and f_s is the sampling frequency of the sub-DACs. In this simulation, the signal bandwidth input to sub-DAC is at most $f_s/2$. We give $F_{BW} = 3\,f_s/2$, and the final output band $F_{BW}{}'$ is $0.9F_{BW}$.

We use two types of inputs; one is an impulse signal to obtain the amplitude and phase characteristics for frequency. The other is also a 4-tone signal for time-domain waveform comparison. Notice that here the DAC has an infinite word length without quantization error.

The passband ripple of the subband digital filter is 0.2 dB, and its stopband ripple is -80 dB. The analysis digital filter was designed with an FIR filter based on a Kaiser window because the FIR filter is linear phase characteristic and the Kaiser window can change the stopband ripple by changing its parameter. The synthesis analog filter was designed with an elliptic filter, because its stopband can be significantly attenuated in a smaller order than other analog filters. Table 2 shows the orders of the filters used in the simulation. Note that we use two types for all pass filters as compensation of phase-nonlinearity characteristic of smoothing and synthesis analog filters. Because the order is smaller than compensating with one type of filter, and the group delay is also smaller. Since the circuit size is not considered in this paper, their orders are high. High orders

of digital filters may not be a problem, but high order synthesis analog filters would consume much power. If their orders are lower, their transition bands are wider. Its one remedy is to use higher sampling frequency of sub-DACs; the input signal bandwidth to sub-DAC becomes can be extended to be wider and then their transition ranges are allowed to be wider, which leads to the lower orders of their corresponding analog filters.

Table2 Orders of the filters used in simulation

Subband Channel	Digital FIR filter			Digital IIR filter		Analog elliptic filter	
	Subband	Lowpass	Inverse sinc	All-pass (smoothing)	All-pass (Analog bandpass)	Smoothing	Analog bandpass
Ch1	402	-	200	14		13	-
Ch2	402	100	200	14	22	13	20
Ch3	402	100	200	14	20	13	20
Ch4	402	100	200	14	20	13	18

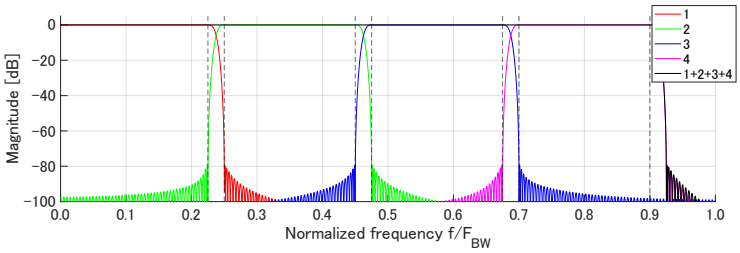

(a) Subband analysis digital filter and their combination

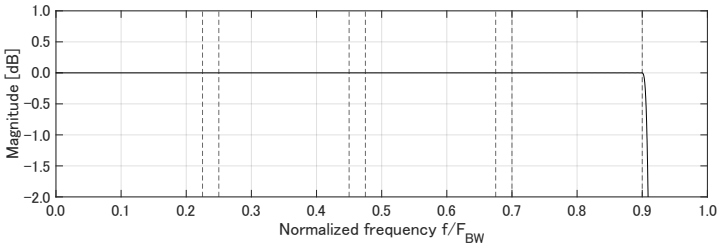

(b) Scaling up the pass band of their combination

Fig. 16. Frequency characteristic of subband analysis digital filters using simulation

Fig. 16 shows the frequency characteristic of subband analysis digital filters. In Fig. 16, (a) shows the filters up to subband channels 1~4 and their combination, and (b) shows scaling up the pass band of their combination. Note that the dotted line in Fig. 16 (b) shows the range where the signal components between subband channels overlap. The signal component is not attenuated inside the dotted line. Following this, the band splitting is performed using these filters.

4.2 Simulation verification by impulse response

Signal attenuation by DAC zero-th order hold output

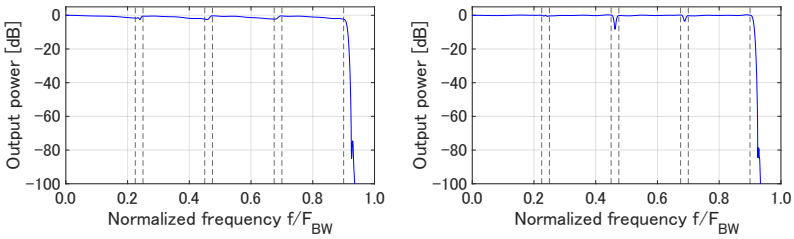

(a) Before compensation **(b) After compensation**

Fig. 17. Simulation results of before and after compensation for the signal attenuation by DAC zero-th order hold output.

Fig. 17 shows the simulation results of before and after compensation for the signal attenuation by zero-th order hold. In Fig. 17, (a) shows the power spectrum without any compensation in Fig. 15, and (b) shows the one with compensation by an inverse sinc filter. In the case of Fig. 17 (a), a zero-th order hold characteristic appears in the signal component of each subband channel. In the case of Fig. 17 (b), the compensation makes the gain to be flat in the entire band of each subband channel. However, since the phase compensation is not performed, the output signal is attenuated inside of the dotted line.

Phase-nonlinearity characteristic of synthesis analog filters

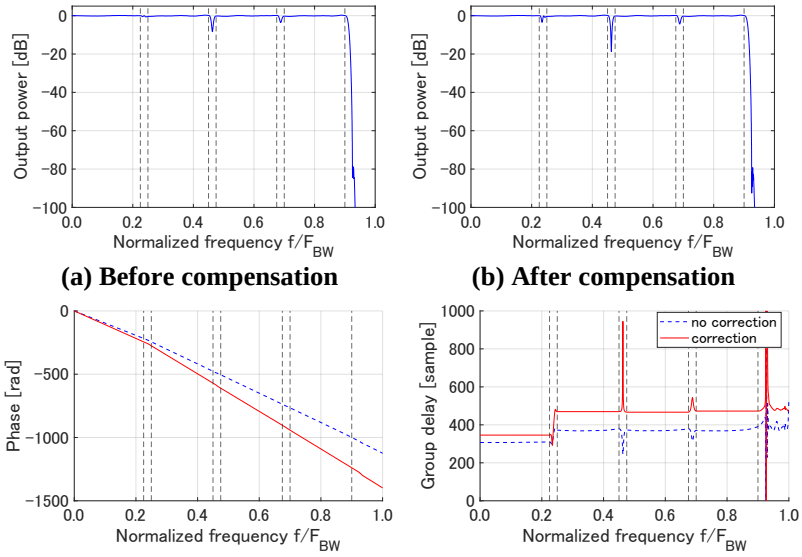

(a) Before compensation **(b) After compensation**

(c) phase characteristic comparison **(d) Group delay comparison**

Fig. 18. Simulation results before and after compensation of phase-nonlinearity characteristic of synthesis analog filters.

Fig. 18 shows the simulation results before and after compensation of phase-nonlinearity characteristic of synthesis analog filters. In Fig. 18, (a) shows the power spectrum with only compensation for signal attenuation by zero-th order hold, and (b) is the one with compensation by all-pass filters, while (c), (d) show the comparison of phase characteristic and group delays in (a) and (b). This simulation is to verify the compensation of phase characteristic, so the power spectrum does not change except inside of the dotted line. As shown in Fig. 18 (d), before the compensation, the group delay for each subband channel is not straight, but curved. On the other hand, after compensation, the group delay is straight. However, the group delays are different among subband channels.

Differences in group delays among subband channels

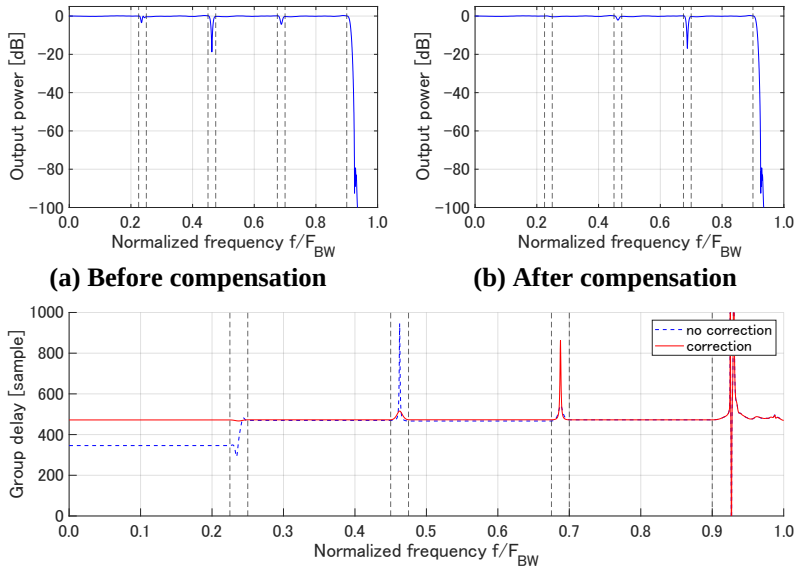

Fig. 19. Simulation results before and after comparison of group delay difference among subband channels.

Fig. 19 shows the simulation results before and after comparison of group delay difference among channels before and after compensation. In Fig. 19, (a) shows the power spectrum with the above two compensations, and (b) is the one in case with compensation by a delay, while (c) is a comparison of the group delays of (a) and (b). Similarly, this is the compensation of phase characteristic, so the power spectrum does not change except inside of the dotted line. As shown in Fig. 19 (c), after compensation, the difference in group delay between among subband channels is reduced substantially. However, since the phases between subband channels do not match, the signal is attenuated inside of the dotted line in Fig. 1.

Phase discontinuity between adjacent subband channels

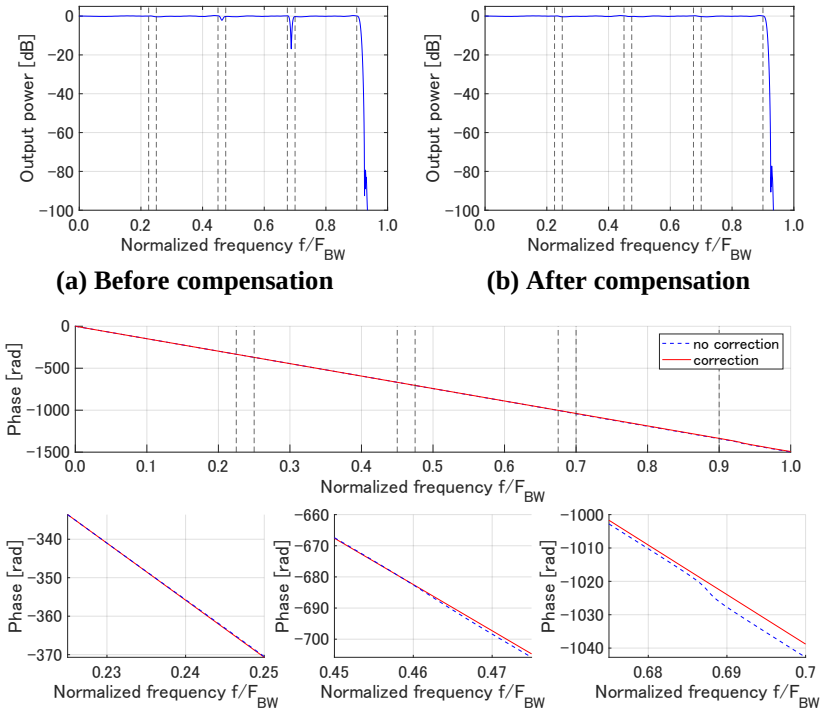

Fig. 20. Simulation results before and after compensation phase discontinuity between adjacent subband channels

Fig. 20 shows the simulation results before and after compensation for the output phase discontinuity between adjacent subband channels. In Fig. 20, (a) shows the power spectrum with the above three compensations, (b) shows the one with the compensation by the initial phase to the carrier signal. (c) shows the comparison of the phase characteristic in (a) and (b). In Fig. 20 (c), the upper figure is the overall phase characteristic, and the lower is the enlarged display inside the dotted line. Before compensation, the power spectrum is attenuated significantly inside the dotted line. As shown in Fig. 20 (c), a large deviation appears in the phase characteristic in this range. After compensation, this deviation disappears, and the power spectrum inside of the dotted line is also not attenuated.

4.3 Simulation verification by 4-tone input signal

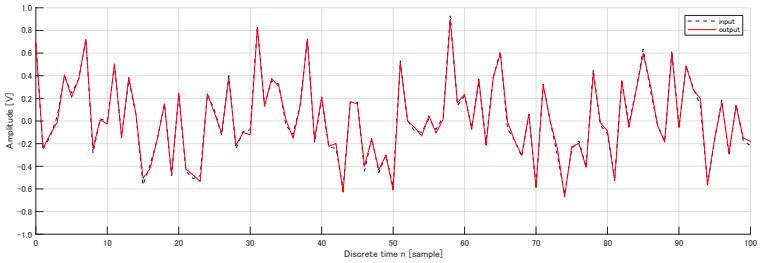

RMSE=0.0254 Vrms
(a) Waveform comparison

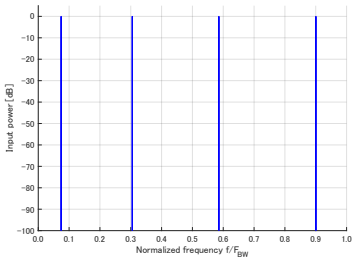

(b) Before compensation

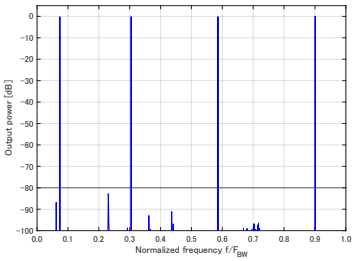

(c) After compensation

Fig. 21. Simulation results using the 4-tone input signal.

Fig. 21 shows the simulation result using the 4-tone input signal to compare the time-domain waveforms. In Fig. 21, (a) shows the input/output waveforms, while (b) and (c) show their power spectrums. In Fig. 21 (a), the RMSE of the output waveform is 0.0254 Vrms, and almost no distortion appears in the output waveform. Then, there are no spurious in the output power spectrum greater than the filter stop band ripple of -80 dB.

5 Conclusion

We have investigated the basic configuration of the frequency interleaved DAC architecture. There the image components by sub-DACs and modulations are generated, and they are removed with the following synthesis analog filters. Besides, these filters have transition bandwidth, and therefore, the input band of each sub-DAC becomes narrow.

We have investigated the subband processing using digital filters for band division. Then, by overlapping the transition band of the filters, the overall DAC output is kept not to be attenuated. To have the input band of the sub-DAC, the frequency shifting and down sampling for its input are performed.

There are several fundamental problems in the above series of processing. The compensation methods for these problems have been discussed. Signal attenuation by zero-th order hold of the sub-DAC output can be compensated by applying an inverse sinc

filter. Phase-nonlinearity characteristic of synthesis analog filters is compensated by applying all-pass filters. Differences in group delay among subband channels are compensated by inserting a delay and changing the sampling timing. Phase discontinuity between adjacent subband channels can be compensated by adjusting the initial phase of the carrier signal in digital signal processing.

We have performed MATLAB simulation, which showed changes in the amplitude and phase characteristic of the signal by compensations. The input and output waveforms were compared, and the validity of the compensation method was verified.

Remaining are compensation methods for circuit implementation issues. For example, we have investigated the compensation for the difference in group delay among subband channels by changing the sampling timing. However, it can only be compensated by delay values that are integer multiples of the sampling period. The group delay of the synthesis analog filter does not necessarily exist within this compensation range, and compensation up to the minute delay cannot be performed. Therefore, it is necessary to compensate for this delay by using analysis digital filters, whose group delay can be adjusted with the time resolution of fractional of the sampling period as described in [19][20]. We will examine circuit implementation issues such as variations in elements during manufacturing, minute delays, nonlinear distortion, and phases of carriers, spurious at inputs, and quantization errors in digital signal processing parts.we will construct their compensation algorithms.

References

1. N. Kurosawa, H, Kobayashi, K. Maruyama, H. Sugawara, K. Kobayashi, “Explicit Analysis of Channel Mismatch Effects in Time-Interleaved ADC Systems”, IEEE Transactions on Circuits Systems—I: Fundamental Theory and Applications, Vol. 48, No. 3, pp. 261-271 (Mar. 2001).
2. R. Kabeya, Y. Umeda, K. Takano, “Frequency-Interleaved ADC with RF Equivalent Ideal Filter for Broadband Optical Communication Receivers”, IEEE International Conference on Electronics, Circuits and Systems, Dubai, United Arab Emirates (Nov. 2021).
3. J. Song, S. Tian, Y. Hen, “Analysis and Correction of Combined Channel Mismatch Effects in Frequency-Interleaved ADCs”, IEEE Transactions on Circuits and Systems–I: Regular Papers, Vol. 66, No. 2, pp. 655-668 (Feb. 2019).
4. K. Asami, K. Kusunoki ,N. Shimizu, Y. Aoki,” Ultra-Wideband Modulation Signal Measurement Using Local Sweep Digitizing Method”, IEEE 38th VLSI Test Symposium, San Diego, CA (April 2020).
5. E. Olieman, A.J. Annema, B. Nauta, A. Bal, P. N. Singh, “A 12b 1.7GS/s Two-Times Interleaved DAC with <-62dBc IM3 Across Nyquist Using a Single 1.2VSupply”, IEEE Asian Solid-State Circuits Conference, Singapore (Nov. 2013).
6. S. Balasubramanian, G. Creech, J. Wilson,S. M. Yoder, J. J. McCue, M. Verhelst, W. Khalil, “Systematic Analysis of Interleaved Digital-to-Analog Converters”,

IEEE Trans. Circuits and Systems-II: Express Briefs, Vol.58, No.12, p882-886 (Dec. 2011).
7. P. J. Pupalaikis, B. Yamrone, R. Delbue, A. S. Khanna, K. Doshi, B. Bhat, A. Sureka, "Technologies for Very High Bandwidth Real-Time Oscilloscopes", IEEE Bipolar/BiCMOS Circuits and Technology Meeting, Coronado, CA (Sept. 2014).
8. C. Schmidt, Interleaving Concepts for Digital-to-Analog Converters: Algorithms, Models, Simulations and Experiments, p99-177, Springer (Jan. 2020).
9. H. Okawara. "Analysis of Pseudo-Interleaving AWG", International Test Conference, Austin, TX (Nov. 2005).
10. J. Deveugele, P. Palmers, M. S. J. Steyaert, "Parallel-Path Digital-to-Analog Converters for Nyquist Signal Generation", IEEE Journal of Solid-State Circuits, Vol. 39, No. 7, p1073-1082 (Jul. 2004).
11. A. Jha, P. R. Kinget, "Wideband Signal Synthesis Using Interleaved Partial-Order Hold Current-Mode Digital-to Analog Converters", IEEE Trans. Circuits and Systems-II: Express Briefs, Vol.55, No.11, pp.1109-1113 (Nov. 2008).
12. C. Schmidt, C. Kottke, V. H. Tanzil, R. freund, V. Jungnickel, F. Gerfers,"Digital-to-Analog Converters Using Frequency Interleaving: Mathematical Framework and Experimental Verification" , Circuits, Systems and Signal Processing 37, pp. 4929-4954 (2018).
13. C. Schmidt, C. Kottke, V. Jungnickel, R. Freund," Enhancing the Bandwidth of DACs by Analog Bandwidth Interleaving", ITG-Fachbericht-Breitbandversorgung in Deutschland, Berlin (Apr. 2016).
14. A. C. Galetto, B. T. Reyes, D. A. Morero, M. R. Hueda, "Background Compensation of Frequency Interleaved DAC for Optical Transceivers", IEEE 12th Latin America Symposium on Circuits and Systems, Arequipa, Peru (Feb. 2021).
15. A. C. Galetto, B. T. Reyes, D. A. Morero, M. R. Hueda, "Adaptive Background Compensation of Frequency Interleaved DACs With Application to Coherent Optical Transceivers", IEEE Access, Vol.9, pp. 41821-41832 (2021).
16. R. E. Crochiere, L. R. Rabiner, Multirate Digital Signal Processing, Prentice-hall Signal Processing Series, Prentice Hall (1996).
17. P. P. Vaidyanathan, "Multirate Digital Filters, Filter Banks, Polyphase Networks, and Applications: A Tutorial", Proc. the IEEE, Vol.78, No.1, pp.56-93 (Jan. 1990).
18. A. Antoniou, Digital Filters: Analysis, Design, and Applications, Second Edition, McGraw-Hill, Inc. (1993).
19. K. Asami, H. Miyajima, T. Kurosawa, T. Tateiwa, H. Kobayashi, "Timing Skew Compensation Technique Using Digital Filter with Novel Linear Phase Condition", IEEE International Test Conference, Austin, TX (Nov. 2010).
20. K. Asami, T. Tateiwa, T. Kurosawa, H. Miyajima, H. Kobayashi, "Digitally-Assisted Compensation Technique for Timing Skew in ATE Systems", IEEE International Mixed-Signals, Sensors, and Systems Test Workshop, Santa Barbara, CA (May 2011).